

AMERICAN ASTRONOMICAL SOCIETY
Division on Dynamical Astronomy
37th Annual Meeting

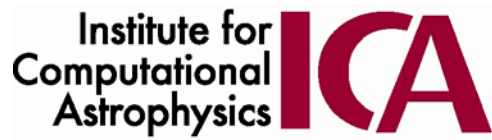


Saint Mary's University
Halifax, Nova Scotia
Canada
June 25 – 29, 2006



McNally Building, Saint Mary's University

The 37th Annual DDA Meeting is sponsored in part by:



37th Meeting of the AAS Division on Dynamical Astronomy
Halifax, Nova Scotia, 25-29 June 2006

Invited talks marked with "I" will be 50 min (40 min + 10 min Q&A)

Contributed talks will be 20 min (15+5)

Oral Sessions are in Sobey Bldg. Rm. 255

Posters, Breakfasts and Coffee Breaks are in Sobey Lobby

Posters will be on display the duration of the meeting.

SUNDAY 25 June	MONDAY 26 June	TUESDAY 27 June	WEDNESDAY 28 June	THURSDAY 29 June
	Continental Breakfast 7:30 - 8:30am	Continental Breakfast 7:30 - 8:30am	Continental Breakfast 7:30 - 8:30am	Continental Breakfast 7:30 - 8:30am
	Welcome and Opening Remarks 8:30 - 8:50 AM	5 Things Every Dynamicist Ought to Know 8:30 - 9:20 AM	10 Extrasolar Planets I 8:30 - 10:00 AM	15 Dynamical Modeling of Orbits 8:30 - 10:20 AM
	1 Small Body Dynamics I 8:50 - 10:20 AM	6 Galactic Structure 9:20 - 11:10 AM		
← 20 minute Coffee Break →				
	2 Small Body Dynamics II 10:40 - 11:40 AM	7 Planetary Ring Systems I 11:30 AM-12:10 PM	11 Extrasolar Planets II 10:20 - 11:20 AM	16 Satellite Dynamics 10:40 - 1:00 PM
← two hour Lunch Break→				Meeting Adjourns 1:00 PM
	3 Planet Formation & Solar System Dynamics 1:40 - 3:00 PM	8 Planetary Ring Systems II 2:10 - 3:50 PM	12 Astrometry and Stellar Systems 1:20 - 3:00 PM	
← 20 minute Break →				
	4 Clusters and the Universe 3:20 - 5:10 PM	9 Brouwer Award Lecture 4:10 - 5:00 PM	13 Captures and Cataclysms 3:20 - 5:00 PM	
Registration Opening Reception 7:00 -10:00 PM Tradewinds Harbour Lounge, Westin Hotel	DDA Business Meeting 5:10 - 6:10 PM	Division Banquet 7:00 PM The Chef's Room	10 minute Break	
			14 Poster Session with refreshments 5:10 - 6:40 PM	

MONDAY

Welcome and Opening Remarks

Monday, June 26, 2006 8:30:00 - 8:50:00 AM

Welcoming remarks will be given by Dr. Terry Murphy, Vice President, Academic & Research, Saint Mary's University. Dr. Joe Hahn, Associate Professor, Department of Astronomy & Physics, Saint Mary's University will brief participants on meeting logistics and agenda.

Oral Session 1 Small Body Dynamics I

Monday, June 26, 2006, 8:50 am - 10:20 am

1.01I Deep Impact: Excavating Comet Tempel 1

Michael F. A'Hearn¹

¹*Univ. of Maryland.*

On 4 July 2005, Deep Impact delivered 19 GJoules of kinetic energy to comet 9P/Tempel 1. On approach, we learned that outbursts by comets are far more common than previously realized and that they can be associated with regions on the surface. We can confidently rule out exogenic sources for these outbursts. Although there are similarities, the geology of the surface is clearly different from that of the few other cometary nuclei visited and very puzzling. There are clearly distinct layers, which are likely not concentric shells but rather discrete blocks. Surface photometric properties are reasonably uniform except in a few small areas.

The impact itself was oblique. Most ejecta were cold, slow-moving, few-micron sized particles. After the first seconds, the ejecta include small crystals of ordinary ice, indicating excavation without heating and thus without chemical alteration. The ejected gases included a large amount of CO₂ and a very large amount of organics in addition to water and species yet unidentified. The refractory to volatile ratio in the ejecta is greater than unity but not dramatically so.

The ejecta enable us to show that the strength of the surface layers, at scales from microscopic to a few hundred meters is remarkably weak and also to show that the bulk density of the nucleus is so low that the entire nucleus must be extremely porous.

This talk will present the current state of our rapidly evolving understanding of comet Tempel 1.

This work was supported by NASA's Discovery Program.

1.02 A Search for Rapidly Rotating Asteroids in the Few-Hundred-Meter Size Range

Thomas S. Statler¹, T. Watanabe²

¹*Ohio Univ.*, ²*St. Mary's University, Canada.*

Rapidly rotating asteroids, with rotation periods under 2 hours, appear abruptly below a diameter of approximately 150 m. Roughly 40 such objects are now known, with periods ranging all the way down to just over one minute. These objects are generally considered to be monolithic, although rubble piles bound by weak cohesion are not ruled out by current data. The cohesive rubble pile model predicts a gradual transition between slow and fast rotators as a function of size; yet currently there is only a single known object (2001 OE84) with a diameter above 200 m and rapid rotation. We will report on initial results from an observational program on the 2.4 m Hiltner telescope at MDM Observatory to search for rapid rotators among NEAs in the 200 m to 1 km size range.

1.03 **The Dynamical Evolution Of Uniformly Rotating Asteroids Subject To Yorp**

Daniel J. Scheeres¹

¹*Univ. of Michigan.*

A detailed derivation is given of the effect of solar radiation on the rotational dynamics of asteroids, commonly called YORP. The current derivation goes beyond previous discussions published in the literature and provides a compact characterization of the effect of YORP by averaging over the rotating body and the asteroid orbit. Using this characterization we present a comprehensive dynamical analysis of the effect of solar radiation torques acting on a uniformly rotating body, and the evolution of its rotation state over time. Our predicted model has the global radiation properties of the asteroid as explicit parameters, and hence can be specified independent of these parameters. Based on our analysis we find that the rotation rate of near Earth asteroids should be subject to large accelerations and decelerations due to YORP, in agreement with previous studies. We analytically show that thermal inertia will have a minor effect on the rotational acceleration and deceleration of a rotating body. Our theory also predicts that asteroid obliquity should have relatively little evolution unless the body is despun to a very slow rotation rate. This is in contrast to previous studies of this effect which predict large changes in obliquity. With this detailed model, in conjunction with estimated asteroid shapes and poles, we compute the expected YORP torques and dynamic response of several asteroids. We also study the change in rotation rate for specific shapes as a function of obliquity.

Oral Session 2 Small Body Dynamics II

Monday, June 26, 2006, 10:40 am - 11:40 am

2.01SP* **A Steady-State Model of NEA Binaries Formed via Tidal Disruption**

Kevin J. Walsh^{1*}, D. C. Richardson¹

¹*Univ. of Maryland.* *Student Stipend Award

We present preliminary results of simulations of steady-state near-Earth asteroid (NEA) binary populations. This study combines the previous work on tidal disruption of gravitational aggregates [Walsh & Richardson 2006, Icarus 180, 201--206] with a Monte Carlo simulation of NEA planetary encounters. Evolutionary effects such as tidally induced binary circularization and widening, as well as binary disruption caused by close planetary encounters, are included. The results show that using the best known distributions of progenitor (small Main Belt asteroid) shape and spin distributions, and current estimates of NEA lifetimes and encounter probabilities, that tidal disruption accounts for approximately 1-5% of NEAs being binaries. Since the observed population is around 15% binaries, there is potentially one or more other important binary formation mechanisms at work. Our work also suggests that even a large pre-existing Main Belt binary population cannot explain the discrepancy. Finally, we present the expected distribution of binary orbital and physical properties for the steady-state population generated by tidal disruption and show that they match well with observations.

2.02 **Binary Asteroids**

Alan W. Harris¹, P. Pravec²

¹*Space Science Inst.*, ²*Czech Academy of Science, Astronomical Institute, Czech Republic.*

There are now nearly 100 binary asteroids known. In the last year alone, 30 binary asteroids have been discovered, half of them by lightcurves showing eclipse events. Similar to eclipsing binary stars, such observations allow determination of orbit period and sizes and shapes of the primary and secondary relative to the orbital dimension. From these parameters one can estimate the mean density of the system, and a number of dynamical properties such as

total specific angular momentum, tidal evolution time scales of spins and orbit, and precession frequencies of the orbit about the primary and of the solar induced “general precession” of the system. We have extracted parameters for all systems with enough observations to allow meaningful determinations. Some preliminary results include: (1) Binaries are roughly as prevalent among small main-belt asteroids as among Near-Earth Asteroids. (2) Most binaries are partially asynchronous, with the secondary synchronized to the orbit period, but the primary still spinning much faster. This is consistent with estimated tidal damping time scales. (3) Most systems have near the critical maximum angular momentum for a single “rubble pile” body, but not much more, and some less. Thus fission appears not to be a viable formation mechanism for all binaries, although near-critical spin rate seems to play a role. (4) Orbits of the secondaries are essentially in the equatorial plane of the primary. Since most primary spins are still fast, the satellites must have been formed into low inclination orbits. (5) Precession frequencies are in the range of the shorter resonance frequencies in the solar system (tens of thousands of years), thus resonance interactions can be expected to have altered spin orientations as systems evolved slowly by tidal friction or other processes. (6) Primaries are unusually spheroidal, which is probably necessary for stability of the binary once formed.

2.03 Relaxed Dynamics of the Trojan Asteroids

Michael Cahill¹

¹*Univ. of Wisconsin, Washington County.*

A statistical theory of gravitationally relaxed linearized Newtonian dynamics for small bodies near $L4$ and $L5$ in the stable case is developed.

It is well known that if n_3 is the angular velocity of the principle bodies and if the z axis is perpendicular to their orbit plane then the z motion equations are $S_3' = n_3 C_3, C_3' = -n_3 S_3$ where $' = d/dt, S_3 = n_3 z, C_3 = z'$.

For the x, y plane there are 2 modes of motion with angular velocities n_1, n_2 obeying $n_1 < n_3 < n_2$ depending on n_3 and the mass ratio m ($m \leq 1/2$) of the principle bodies. Here the motion equations can be written like the z equations as $S_i' = n_i C_i, C_i' = -n_i S_i$ where S_i, C_i are calculated linear combinations of x, x', y, y' .

The mass specific energy for the 3 modes is $e_i = 1/2 C_i^2 + 1/2 S_i^2$, and is constant implying that the phase point of a small body moves steadily in a circle in the (C_i, S_i) plane.

If gravitational relaxation holds then a kinematic form of 6 dimensional Eherenfest phase space may be used for each small body: $\{C_1, S_1, C_2, S_2, C_3, S_3\}$. It will be shown that the appropriate specific energy e on which a particle probability distribution depends is the total of the mode specific energies, $e = e_1 + e_2 + e_3$ which is not the specific Jacobi integral to 2nd order.

Most probable statistics and microcanonical statistics imply that the distribution is given as a function of N , the total population of small bodies and a dimensionless specific energy ϵ , $\epsilon = 3e / \langle e \rangle$ where $\langle e \rangle$ is the average energy. Then to lowest order in N the probability distribution ψ is $d\psi = k(Ne^{-\epsilon} - 1)\epsilon^2 d\epsilon$ for $\epsilon \leq \epsilon_c$, and $d\psi = 0$ for $\epsilon_c \leq \epsilon$ where ϵ_c is the specific energy cutoff given by $\epsilon_c = \ln(N)$ and where k is the distribution normalization constant.

A fitting of the Minor Planet Center data for the Jovian Trojans to this distribution will be given at the 2006 DDA meeting.

Oral Session 3 Planet Formation & Solar System Dynamics

Monday, June 26, 2006, 1:40 pm - 3:00 pm

3.01 Outer Solar System on the Edge of Chaos

Wayne B. Hayes¹

¹*UC, Irvine.*

The existence of chaos among the system of Jovian planets (Jupiter, Saturn, Uranus, and Neptune) is not yet firmly established. Although Laskar originally found no chaos in the outer Solar System, his “averaged” integrations did not account for the possibility of mean-motion resonances. Once full n-body integrations were performed, a dichotomy arose. On one hand, many investigators (Sussman, Wisdom, Murray, Holman, among many others) consistently measured a Lyapunov time of between 5 and 12 million years in the outer Solar System; the chaos can even be explained as the overlap of three-body resonances (Murray + Holman, *Science* 283, 1999). Furthermore, Murray + Holman’s theory has been recently corroborated across a wide range of system parameters (Guzzo 2005), and the chaos does not disappear with decreasing timestep. On the other hand, some other investigators (Newman, Graziar, and Varadi, among several others) have compelling evidence against chaos. Namely, they have convincingly demonstrated that a symplectic integration using the famous Wisdom + Holman (1992) symplectic mapping with a 400-day timestep reproduces the chaos seen by others, but that the chaos disappears and the orbit converges to being regular as the timestep decreases. Their integration remains regular, showing beautiful convergence with decreasing timestep, down to a 2 day timestep.

The resolution of this apparent paradox is simple. The orbital positions of the Jovian planets is known only to a few parts in 10⁷, and it turns out that within that observational error ball, there exist both chaotic and regular solutions. I will demonstrate this fact using several initial conditions and several accurate integration algorithms. Thus, whether a particular investigator will see chaos or not depends (essentially randomly) upon the details of how that investigator draws their initial conditions. Thus, some investigators legitimately find chaos, while others legitimately find no chaos.

3.02 Giant Planet Accretion And Migration: Surviving The Type I Regime

Edward Thommes¹, N. Murray¹

¹*CITA, Canada.*

In the core accretion model of gas giant planet formation, a large solid core about 10X the Earth’s mass forms first, then accumulates its massive envelope (~100 or more Earth masses) of gas. However, inward planet migration due to gravitational interaction with the proto-stellar gas disk poses a big hazard in this model. Core-sized bodies undergo rapid “type I” migration; for typical parameters their migration timescale is much shorter than their accretion timescale. How, then, do growing cores avoid spiraling into the central star before they ever get the chance to become gas giants? I will present a simple model of core formation in a gas disk which is viscously evolving. It turns out that as the disk accretes onto the star, a window of opportunity for successful core growth may open. I will discuss what implications this model has for the link between disk properties and the likelihood of forming gas giants.

3.03 Direct Simulations of Growth from 1 km Planetesimals at 0.4 AU

Rory Barnes¹, T. R. Quinn², J. J. Lissauer³, D. C. Richardson⁴

¹*Univ. Of Arizona,* ²*Univ. Of Washington,* ³*NASA Ames,* ⁴*Univ. Of Maryland.*

We present results of N-body simulations of planetesimal accretion beginning with 1 km-sized particles in orbit about a 1 solar mass star at 0.4 AU. Such particles may be the fundamental building blocks of terrestrial planets. This initial disk of planetesimals contains far too many bodies for any current N-body code to integrate, and we therefore only model a sample patch of the disk. Although this greatly reduces the number of bodies, our principal simulation still tracks over 100,000 particles in this manner. We consider several plausible initial conditions and monitor the growth of these particles. Our simulations use the perfect accretion model; planetesimal collisions are assumed to be completely inelastic. We integrate one patch for almost 1000 orbits and follow mass growth for over three orders of magnitude (the largest particle at the end of this simulation has a radius of over 12 km). Additionally, the escape speed of the largest particle grows considerably faster than the velocity dispersion of particles, suggesting impending runaway growth, although it is yet to begin in our simulations.

3.04 Particle-Laden Turbulence from the Streaming Instability

Andrew Youdin¹, A. Johansen²

¹Princeton Univ., ²MPIA Heidelberg, Germany.

I will present recent work on a novel and robust type of turbulence which arises spontaneously in protoplanetary disks due to the drag forces between particles and gas. This “particle laden” turbulence is driven by the amplification of the streaming instability identified by Youdin & Goodman (2005). The physics of this system is considerably simpler than the well-known vertical shear (or Kelvin-Helmholtz) instability, allowing us to isolate the role of aerodynamic coupling. The nonlinear behavior is studied with a hydrodynamics code to simulate the gas and N-body particle integrations for the solids. Even in the absence of self-gravity we find that particle clumping is energetically favored. The relevance of particle overdensities, and other aspects of the turbulent flow, to planetesimal formation will be discussed.

Oral Session 4 Clusters and the Universe Monday, June 26, 2006, 3:20 pm - 5:10 pm

4.011 On the Cusp of the Dark Matter

Hugh M. Couchman¹

¹McMaster Univ., Canada.

The Lambda cold dark matter cosmology, now strongly constrained by direct observation at early epochs, successfully describes the structure of the evolved universe on large and intermediate scales but suffers serious difficulties on smaller, galactic scales. Among the significant problems is a persistent discrepancy between observations of nearby galaxies, which imply that galactic dark matter haloes have flat cores, and the cosmological model, which predicts that the haloes should have a central density cusp. Using N-body simulations we show that random bulk gas motions in small primordial galaxies, of the magnitude expected in these systems, result in a flattening of the central dark matter cusp on short timescales (of order 100 million years). Gas bulk motions in early galaxies are driven by supernova explosions and stellar winds which result from ongoing star formation. During the subsequent evolution, most of the galactic gas will be consumed by star formation and lost via galactic winds, leaving a gas content in agreement with observations of present-day galaxies. Our mechanism is general and would have operated in all star-forming galaxies at redshifts > 10 . Once removed, the cusp cannot be reintroduced during the subsequent merger hierarchy involved in building larger galaxies. As a consequence, in the present universe both small and large galaxies would have flat dark matter core density profiles, in agreement with observations.

Support from NSERC, The Canadian Institute for Advanced Research and SHARCNET is gratefully acknowledged.

4.02 Orbits In Extended Mass Distributions: General Results And The Spirographic Approximation

Fred C. Adams¹, A. M. Bloch¹

¹Univ. of Michigan.

This talk explores orbits in extended mass distributions and develops an analytic approximation scheme based on epicycloids (spirograph patterns). We focus on the Hernquist potential $\Psi = 1/(1 + \xi)$, which provides a good model for many astrophysical systems, including elliptical galaxies (with an $R^{1/4}$ law), dark matter halos (where N-body simulations indicate a nearly universal density profile), and young embedded star clusters (with gas density $\rho \propto 1/\xi$). For a given potential, one can readily calculate orbital solutions as a function of energy and angular momentum using numerical methods. In contrast, this work presents a number of analytic results for the Hernquist potential and proves a series of general constraints showing that orbits have similar properties for any extended mass

distribution (including, e.g., the NFW profile). We discuss circular orbits, radial orbits, zero energy orbits, different definitions of eccentricity, analogs of Kepler's law, the definition of orbital elements, and the relation of these orbits to spirograph patterns (epicycloids). Over a large portion of parameter space, the orbits can be adequately described (with accuracy better than 10%) using the parametric equations of epicycloids, thereby providing an analytic description of the orbits. As an application of this formal development, we find a solution for the orbit of the Large Magellanic Cloud in the potential of our Galaxy.

4.03 **Simulating the Production of Intracluster Light**

Craig Rudick¹

¹*Case Western Reserve University.*

Using N-body simulations, we have modeled the production and evolution of diffuse, low surface brightness intracluster light (ICL) in galaxy clusters. Using an observational definition of ICL to be luminosity at V-band surface brightness of greater than 26.5 magnitudes per square arcsecond, we have found that the fraction of cluster luminosity contained in ICL generally increases as clusters evolve, although there are large deviations from this trend over short timescales, including sustained periods of decreasing ICL luminosity. Most ICL luminosity increases come in short, discrete events which are highly correlated with group accretion events within the cluster. Additionally, the morphological structure of the ICL changes with time, evolving from a complex of filaments and small-scale, relatively high surface brightness features early in a cluster's history, to a more diffuse and amorphous cluster-scale ICL envelope at later times.

4.04 **Dwarf Spheroidals - Hotbed of Dark Matter or Test Bed of New Physics?**

David F. Bartlett¹

¹*Univ. of Colorado.*

For many years, the dozen or so dSph's orbiting the Milky Way have been accused of harboring large (and varying) amounts of dark matter. How else can one explain the large dispersion in radial velocities observed within a single dSph? Newtonian tidal forces from the Milky Way itself are not helpful. These fall off as $1/R^3$ and are insignificant at the $R \approx 100$ kpc distances to the spheroidals.

The situation is entirely different with the sinusoidal potential. Sinusoidal gravity is a newly postulated replacement for dark matter (and dark energy).[1] Here the gravitational potential is alternately attractive and repulsive, with a universal wavelength determined empirically to be

$\lambda_0 = R_0 / 20 \approx 400$ pc.[1] . The potential from a point mass is $\phi(R) = -(GM/R) \cos[2\pi R/\lambda_0]$. When $R \gg \lambda_0$, the potential resembles that of a (static) spherical wave. The potential, force, and tidal force ($\phi(R)$, $g(R)$, and $dg(R)/dR$) all fall off simply as $1/R$. Not surprisingly, for extended mass distributions, Poisson's equation is replaced by one that could have been written by Helmholtz: $\Delta\phi + (2\pi/\lambda_0)^2 \phi = 4\pi\rho$.

At large distances from the Galaxy, the potential separates as a spherical wave should, into an angular part and a radial one: $\phi(R,b,l) = \Psi(b,l) \cos[2\pi R/\lambda_0] / R$. Here I will show why, surprisingly, the central bar of the galaxy is a dominant contributor to $\Psi(b,l)$. I also will present evidence from existing observations showing that the central bar is important for the dSph's and will make predictions for future observations.

[1] D.F. Bartlett. "Analogies between electricity and gravity", *Metrologia* 41, S115-S124 (2004). "Cosmology & the Sinusoidal Potential", AAS-208, Calgary, June, 2006.

DDA Business Meeting, Monday, June 26, 2006 5:10:00 - 6:10:00 PM

TUESDAY

Invited Session 5 Things Every Dynamicist Ought to Know

Tuesday, June 27, 2006, 8:30 am - 9:20 am

5.01I Secular Resonances In Planetary Systems

Renu Malhotra¹

¹*Univ. of Arizona.*

Secular effects introduce very low frequencies in planetary systems. The consequences are quite varied. They include mundane effects on the planetary ephemerides and on Earthly seasons, but also more esoteric effects such as apsidal alignment or anti-alignment, fine-splitting of mean motion resonances, broadening of chaotic zones, and dramatic orbital instabilities. Secular effects may shape the overall architecture of mature planetary systems by determining the long term stability of major and minor planetary bodies. This talk will be partly tutorial and partly a review of secular resonance phenomena here in the solar system and elsewhere in extra-solar systems.

I acknowledge research support from NASA-Origins of Solar Systems and NASA-Outer Planets research programs.

Oral Session 6 Galactic Structure

Tuesday, June 27, 2006, 9:20 am - 11:10 am

6.01I Galactic Structure and Dynamics with Tidal Streams

Steven R. Majewski¹

¹*Univ. of Virginia.*

Recent detailed investigations revealing substantial substructure in the distribution and dynamics of stars in the Galactic halo would seem to be bearing out the basic tenets of standard LCDM models of the hierarchical growth of galaxies in the universe; yet some apparent discrepancies between the models and observations remain. The discovery and mapping of long, coherent streams of tidal debris from disrupted Galactic satellites enables new tests of the standard structural evolution models. Apart from their obvious usefulness in demonstrating in detail the hierarchical growth of the Milky Way, the dynamical coldness and coherence of halo tidal streams make them sensitive probes of the Galactic potential, and can be used to measure its shape, lumpiness and strength. The addition of valuable proper motion data from future space-based astrometric missions, like SIM Planetquest, will dramatically increase the sensitivity of tidal streams as dynamical probes.

6.02 On Raising A Globular Cluster Formed In The Galactic Disk Into The Halo

Kimmo A. Innanen¹

¹*York Univ., Canada.*

Classically, most globular clusters (GC's) are thought to have formed in situ in a galaxy's halo. An alternative possibility is examined in an approximate, empirical way. An axisymmetric galactic model is constructed with simple, multiple resonances in the solar vicinity (galactic year, epicyclic period, vertical period). A resonant internal bar or distortion stirs the resonances so as to break the action of the third (quasi) integral that otherwise restricts the orbit to a low-inclination box. Initial computations indicate that the orbits of GC's and stars formed in the disk with low

angular momentum become chaotic and gradually rise into the halo where they subsequently spend most of their time. An n-body simulation will be required to establish this result in a self-consistent way. Other implications are mentioned. This research was supported NSERC.

6.03SP* Radial Heating of a Galactic Disk by Multiple Spiral Density Waves

Ivan Minchev^{1*}, A. Quillen¹

¹*University of Rochester.* *Student Stipend Award

We consider a differentially rotating, 2D stellar disk perturbed by two steady state spiral density waves moving at different pattern speeds. Our investigation is based on direct numerical integration of initially circular test-particle orbits. We examine a range of spiral strengths and spiral speeds and show that stars in this time dependent gravitational field can be heated (their random motions increased). This is particularly noticeable in the simultaneous propagation of a two-armed spiral density wave near the corotation resonance (CR), and a weak four-armed one near the inner and outer 4:1 Lindblad resonances. In simulations with two spiral waves moving at different pattern speeds we find: (1) the variance of the radial velocity, $(\sigma_R)^2$, exceeds the sum of the variances measured from simulations with each individual pattern; (2) $(\sigma_R)^2$ can grow with time throughout the entire simulation; (3) $(\sigma_R)^2$ is increased over a wider range of radii compared to that seen with one spiral pattern; (4) particles diffuse radially in real space whereas they don't when only one spiral density wave is present. Near the CR with the stronger, two-armed pattern, test particles are observed to migrate radially. These effects take place at or near resonances of both spirals so we interpret them as the result of stochastic motions. This provides a possible new mechanism for increasing the stellar velocity dispersion in galactic disks. If multiple spiral patterns are present in the Galaxy we predict that there should be large variations in the stellar velocity dispersion as a function of radius.

6.04 Phase Space Structure in the Solar Neighbourhood

Dalia Chakrabarty¹

¹*University of Nottingham, United Kingdom.*

This work is an attempt to model the local phase space structure of the disk of our Galaxy, as sculpted by the central bar and a tightly wound, 4-armed outer spiral pattern, that are invoked to perturb a warm quasi-exponential model galactic disk. The recovered velocity distributions are compared to the velocity diagram obtained from the Hipparcos observations. Particular emphasis is given to the reproduction of the moving groups that have been identified in the solar neighborhood. Sample distributions will be presented to

illustrate the success of the "good" models. Besides, we will discuss the formulation of a goodness of fit analysis that checks the likelihood that the observed data is drawn from a model distribution; this is performed in terms of the p-value of a test statistic. Distributions of this goodness of fit parameter, over the studied range of radius and azimuth will be presented for each distinct

simulation: bar only; spiral only; bar and spiral, with varying ratios between their pattern speeds. The locations within this range that correspond to the "good" models are identified with the aim of extracting important dynamical quantities, namely the bar angle and pattern speed. It is found that while this approach is a neat way of estimating the bar parameters, it fails in the case when the spiral pattern is used alone, or when the pattern speeds are chosen to render the ILR of the spiral coincident with the physical location of the OLR of the bar. The dynamical origin of this behaviour and its implications will be discussed. A brief discussion of the orbits in the case of the bar-only and spiral-only perturbations will also be included. I wish to acknowledge the support of a Royal Society Dorothy Hodgkin Research Fellowship.

Oral Session 7 Planetary Ring Systems I
Tuesday, June 27, 2006, 11:30 am - 12:10 pm

7.01 Outer Rings and Chaotic Orbits in the Uranian System

Mark R. Showalter¹, J. J. Lissauer², I. de Pater³

¹SETI Institute, ²NASA/Ames Research Center, ³U. C. Berkeley.

Hubble observations of the Uranian system, spanning 2003 to the present, have revealed two small regular satellites and two faint, outer rings. The satellite Mab (U XXVI) is ~ 12 km in radius and orbits 97,735 km from the center of Uranus, between the orbits of Puck and Miranda. It shows a significant, unexplained orbital libration; its mean longitude in 2004 fell 1° behind that in 2003 and 2005. Cupid (U XXVII) is ~ 9 km in radius and orbits at 74,392 km, just 863 km interior to the orbit of Belinda. These moons are locked in 44:43 resonance. Most of the other inner moons Belinda through Portia show measurable orbital changes in the last 20 years, suggesting subtle, possibly chaotic interactions.

Both newly-discovered rings have been recovered from high-phase Voyager images, and photometry indicates that they are composed primarily of dust. Peak normal optical depths are $\sim 10^{-5}$. Ring R/2003 U 1 peaks at the orbit of Mab and is almost certainly produced by dust ejected from Mab's surface. It has a triangular profile with a full width of $\sim 20,000$ km. R/2003 U 2 orbits at 67,300 km, and is bounded by the orbits of nearby Portia and Rosalind. No known moons fall within this region; we hypothesize that a belt of embedded, sub-km bodies serve as the unseen source of this dust. Recent Keck observations reveal that the inner ring is red but the outer ring is blue. Blue indicates that particle sizes are primarily sub- μm in size; the dynamical implications of this result are not currently understood.

Support for this publication was provided by NASA through proposals GO-9823, GO-10102, and GO-10274 from the Space Telescope Science Institute, which is operated by the Association of Universities for Research in Astronomy under NASA contract NAS5-26555.

7.02 Shapes and Kinematics of Eccentric Features in Saturn's C Ring and Cassini Division

Joseph Spitale¹, C. C. Porco¹

¹Space Science Institute.

Using high-resolution movies and azimuthal imaging scans with radial scales as fine as a few km and longitudinal resolutions as fine as a fraction of a degree, we examine the shapes and kinematics of a number of noncircular features in Saturn's rings.

In the C ring, the Maxwell ringlet, at 1.45 R_s , is consistent with a freely-precessing Keplerian ellipse whose inner and outer edge apsides are aligned. The 1.470- R_s ringlet shows about 5 km of scatter about a mean semimajor axis, but no coherent pattern is discernible. The 1.495- R_s ringlet shows residuals of about 5 km about a mean semimajor axis, but appears more complicated than a freely-precessing ellipse.

The B-ring outer edge shows the expected two-lobed shape rotating with the mean motion of Mimas, but with periape leading the satellite by about 28 deg. That $m=2$ solution yields high residuals, which might be explained by a three-lobed pattern rotating at about 505.5 deg/day. In addition to the dominant $m=1$ eccentric, freely-precessing elliptical mode, the multi-mode Huygens ringlet also shows an $m=2$ shape with a pattern speed equal to, and phase almost exactly opposite to, that of the B-ring outer edge, suggesting that it is influenced not only by Mimas, but perhaps also by the outer B-ring. There may also be an $m=6$ mode precessing at about 631 deg/day.

Oral Session 8 Planetary Ring Systems II
Tuesday, June 27, 2006, 2:10 pm - 3:50 pm

8.01 Brightness Asymmetries in Saturn's Rings

Richard G. French¹, H. Salo², C. McGhee¹, L. Dones³

¹Wellesley College, ²U. of Oulu, Finland, ³SWRI.

The well-known quadrupole brightness asymmetry of Saturn's rings is a natural consequence of the competition between the tendency of particles to clump gravitationally and the frustration of this process by tidal shearing interior to the Roche limit. The resulting Julian-Toomre wake structures are tilted by about 23 degrees relative to circular ring features, and when viewed along their length, the rings appear dimmer because ring particles hide each other and more of the dark sky is visible between particle streams. We present an overview of the brightness asymmetries detected in the A and B rings from a decade of Hubble Space Telescope UBVRI images obtained with WFPC2 over a full Saturn season, spanning the full range of solar phase angles accessible from the Earth images. We have developed dynamical models for gravity wakes and photometric procedures to calculate the resultant wake-driven brightness asymmetry for any given illumination and viewing geometry. We examine the detailed dependence of the asymmetry amplitude and longitude of minimum brightness on elevation angle, solar phase angle, and wavelength.

For example, the phase angle and wavelength dependence helps to distinguish between the single and multiple scattering contributions to the observed brightness, as stronger asymmetry is expected in multiply-scattered light. Similarly, the variation of asymmetry amplitude with ring opening angle is highly sensitive to the vertical structure of rings. Finally, we examine the radial variations of the strength of the asymmetry, and explore the dependence on ring optical depth, density wave activity, and the strength of keplerian shear. This work was supported in part by the NSF and by the NASA PG&G program.

8.02 Shock Wave Dynamics in Planetary Rings

Glen R. Stewart¹

¹Univ. of Colorado.

Previously published models of nonlinear density waves and nonlinear satellite wakes in planetary rings have been based upon approximate solutions of kinetic equations or fluid models (Borderies et al. 1985, 1986 and Shu et al. 1985). Both of these research groups admitted it was difficult for their models to reproduce the short damping lengths that are observed for most density waves in Saturn's rings. The models also have difficulty explaining the amplitude and wavelength of the first two wave peaks in observed nonlinear density waves. Recent N-body simulations of nonlinear satellite wakes demonstrate that collisional damping in the wake peaks is enhanced by vertical splashing of particles associated with a loss of hydrostatic equilibrium in the vertical direction (Lewis and Stewart 2000). I will describe a new fluid model for nonlinear waves in planetary rings that includes deviations from hydrostatic equilibrium in the vertical direction. I will also show how collisional damping in nonlinear waves can be modeled as discontinuous shocks that abruptly decrease the orbital eccentricities of the particle orbits in the wave. Abrupt changes in the particle's semimajor axes must also occur in these shocks because the radial distance from Saturn does not change in an idealized shock.

8.03 Cassini-VIMS Observations Of Self-gravity Wakes In Saturn's Rings

Philip D. Nicholson¹, M. M. Hedman¹, Cassini-VIMS Team

¹*Cornell Univ.*

Between May 24 and August 9, 2005 Cassini's Visual and Infrared Mapping Spectrometer (VIMS) observed four occultations of the long-period variable star, α Ceti (Mira) by Saturn's rings. Large, systematic variations in the transmission of the A ring with longitude are evident in the data, with a maximum in transmission occurring at a longitude of $\sim 250^\circ$ relative to the observer. This is consistent both with the well-known azimuthal asymmetry in reflected light from the A ring, and with numerical models of spontaneous gravitational wakes (e.g., Salo et al. 2004). The physics underlying such wakes is essentially the same as the "swing amplifier" which was studied in the context of galactic disks by Julian & Toomre (1966) and Toomre & Kalnajs (1991).

We have developed a simple model of transmission through a set of parallel wakes, modelled as opaque cylinders with elliptical cross-sections. By fitting the predictions of this model to the observed variations of transmission with longitude, we find the following. (1) The orientation of the wakes varies slightly but systematically across the A ring, from 18° to 26° relative to the azimuthal direction. (2) The peak transmission reaches a maximum in the middle A ring at a radius of 129,000 km, in good agreement with the radius of minimum reflected brightness seen in the Voyager images by Dones et al. (1993). (3) Both the orientation and peak transmission vary anomalously in the vicinity of strong density waves. (4) The width of the transmission peak implies an average vertical thickness for the wakes, H , which varies from 9-12% of the wake wavelength, λ . On the assumption that λ is given by Toomre's critical wavelength for axisymmetric instability in a self-gravitating disk, $4\pi^2 G\sigma\Omega^2$, we estimate an effective ring thickness of ~ 5 m.

Supported by NASA and the Cassini-Huygens Project.

8.04 Disk Response to Variable Forcing: The Rings and Co-orbital Satellites of Saturn

Matthew S. Tiscareno¹, P. D. Nicholson¹, J. A. Burns¹, M. M. Hedman¹, C. C. Porco²

¹*Cornell Univ.*, ²*Space Science Institute.*

Density waves raised in Saturn's rings at inner Lindblad resonances (ILRs) with the co-orbital satellites Janus and Epimetheus have an unusual and complex structure, making their interpretation difficult. High-resolution Cassini images have revealed much new detail not only of the waves raised at first-order ILRs, but also at second-order and even third-order ILRs. Because the latter resonances are weaker, the induced density perturbations are much smaller than the background density, allowing linear superposition of overlapping waves.

Janus and Epimetheus are in a mutual horseshoe configuration; as they orbit Saturn, one satellite is slightly inward of the other, but they effectively switch places every 4 years. In some regions of the rings, the low group velocity yields a density wave propagation time that is comparable to the period of the satellites' libration.

We propose that the complex co-orbital density wave morphology can be explained by the superposition of multiple wave segments, starting and stopping at different locations as the satellite forcing changes, and propagating outwards with group velocities as low as 6 km/yr. We will present preliminary results from a linear model, along with supporting evidence from wavelet analysis of Cassini images that substantiates our claim.

8.05 Remarkably Regular Ripples in Saturn's Dynamic D Ring

Joseph A. Burns¹, M. Hedman¹, M. Tiscareno¹, P. Nicholson¹, M. Showalter², A. Bosh³, C. Porco⁴
¹Cornell Univ., ²SETI Institute, ³Boston U. at Lowell Observatory, ⁴CICLOPS, Space Science Institute.

Cassini observations are revealing that Saturn's closest ring, its D ring, has changed significantly since Voyager's era. Furthermore, this ring also exhibits unusual phase behavior and, in places, its morphology is difficult to interpret. Here we focus on structures in the outermost D region (73,200 - 74,000 km), just interior to the C ring. A regular pattern with a wavelength of ~30 km observed across this region can be attributed to a thin, vertically corrugated ring with a wave height of a few km, viewed at low elevation. A similar pattern was also found during a shallow-elevation (2.7 σ) stellar occultation on 21-22 November 1995, but then a wavelength of ~60 km was present. The wavelength thus seems to shorten with time; the time-separated Cassini observations confirm that the wavenumber increases temporally at a rate 2.54 (+/-0.02) x10⁻⁵/km/day. This rate is consistent with differential nodal regression of an initially thin, slightly inclined ring. The differential regression also seems to be faster closer to the planet, as expected if due to higher-order gravity terms. Because Saturn is so near the D ring, many J_{2n} affect the regression rate. Given the radial distance across this structure, one can place strong constraints on a combination of Saturn's J_{2n}, including terms with n > 10, by watching the wave pattern tighten during the remaining years of the Cassini mission. Unwinding the corrugated spiral backwards in time indicates that this region of the D ring was a simple inclined sheet in the year 1984. We propose that a comet or meteoroid may have collided with the D ring at this time, disrupting a D-ring parent body and slightly tilting the angular momentum of the system.

Invited Session 9 Brouwer Award Lecture **Tuesday, June 27, 2006, 4:10 pm - 5:00 pm**

9.011 Lunar Laser Ranging and the Evolution of Lunar Dynamics

James G. Williams¹
¹JPL.

The shift from angular positions of the Moon to laser ranges required changes in concept as well as data analysis for Earth-Moon dynamics. With angular positions, the emphasis is on the motion of the lunar center of mass. With ranges, the locations of the tracking stations and laser retroreflectors and the orientation of the Earth and Moon become equally important. With angular positions, the distance affects angles through the parallax, while the lunar orbital angular components affect range through projection effects. For calculating the orbit and physical librations for data analysis, range accuracy encouraged a shift from series representations to numerical integration. However, series representations provide insight and have special applications such as frequency dependent tidal effects. Lunar ranging started in 1969 and there have been important subsequent improvements in range accuracy. Over the same time span, the geometrical and dynamical models have become more complex improving the rms fits more than two orders of magnitude. The benefit of accurate ranges and model complexity is the increased number of solution parameters which can be recovered from the fits. Those parameters include precession and tidal dissipation plus station positions and motions for the Earth, gravitational physics tests of equivalence principle and dG/dt from the orbit, and solid-body tides and fluid-core/solid-mantle interactions for the Moon. The range quality and model capabilities have been linked in the past and improved future data and models should bring new results.

Division Banquet, The Chef's Room **Tuesday, June 27, 2006 7:00:00 PM**

Banquet Keynote Speaker: Dr. John Reid, Department of History at Saint Mary's University. The title of Dr. Reid's talk is: "1606 and All That: Misery and Good Cheer in the History of Atlantic Canada."

WEDNESDAY

Oral Session 10 Extrasolar Planets I

Sobey Bldg. Rm. 255

Wednesday, June 28, 2006, 8:30 am - 10:00 am

10.01I Observed Properties of Multi-Planet Systems

Geoffrey W. Marcy¹

¹*UC, Berkeley.*

We present the properties of the 21 multiple-planet systems that have well defined orbital parameters and minimum masses. The parameters have been updated with the latest Doppler measurements. We present two new multiple-planet systems, one having two short period planets and the other with a short period and decade-long second planet. The fraction of known planet-bearing stars that contain additional giant planets is 13%. Clear evidence of mean-motion resonances is found in 4 of 21 of the multiple-planet systems, and several other systems may also reside in resonances, requiring dynamical analysis. Apparently, migration and dynamical evolution of within planetary systems commonly results in resonance capture. The common occurrence of orbital eccentricities ($e > 0.1$) may also stem from planet-planet interactions, often resulting in an ejected planet. Many stars having only one planet have Doppler measurements that hint at additional, long-period planets, providing a glimpse of the occurrence of planets beyond 5 AU.

10.02 Detection of Terrestrial Planets in the Habitable Zones of Nearby Stars with SIM PlanetQuest

Joseph Catanzarite¹, M. Shao¹, A. Tanner¹, S. Unwin¹, J. Yu¹

¹*JPL.*

SIM (Space Interferometry Mission) PlanetQuest is a space-borne Michelson interferometer for precision stellar astrometry, with a nine meter baseline, currently slated for launch in 2015. One of the principal science goals is the astrometric detection and orbit characterization of terrestrial planets in the habitable zones of nearby stars. Differential astrometry of the target star against a set of reference stars lying within a degree will allow measurement of the target star's reflex motion with astrometric accuracy of 1 micro-arcsecond in a single measurement.

We present a quantitative assessment of SIM's capability for detection of terrestrial planets in the habitable zones of nearby solar-type stars. Note that the orbital periods of these planets are generally shorter than the five-year SIM mission. We formulate a joint periodogram as a tool for planet detection from astrometric data. For adequately sampled orbits, i.e., five or more observations per period, over a sampling timespan longer than the orbit period, we find that the joint periodogram is more sensitive than the chi-squared test for the null hypothesis.

In our analysis of the problem, we use Monte Carlo simulations of orbit detection, together with realistic observing scenarios, actual target and reference star lists, realistic estimates of SIM instrument performance and plausible distributions of planetary system parameters.

Performance is quantified by three metrics: minimum detectable planet mass, number and mass distribution of detected planets, and completeness of detections in each mass range. We compare SIM's performance on target lists optimized for the SIM and Terrestrial Planet Finder Coronagraph (TPF-C) missions.

Finally, we discuss the issue of confidence in detections and non-detections, and show how information from SIM's planet survey can enable TPF to increase its yield of terrestrial planets.

This work was carried out at the Jet Propulsion Laboratory, California Institute of Technology, under contract with NASA.

10.03 Predictions For A Planet Just Inside Fomalhaut's Eccentric Ring

Alice C. Quillen¹

¹*Univ. of Rochester.*

We propose that the eccentricity and sharpness of the edge of Fomalhaut's disk are due to a planet just interior to the ring edge. The collision timescale consistent with the disk opacity is long enough that spiral density waves cannot be driven near the planet. The ring edge is likely to be located at the boundary of a chaotic zone in the corotation region of the planet. We find that this zone can open a gap in a particle disk as long as the collision timescale exceeds the removal or ejection timescale in the zone. The ring edge has eccentricity caused by secular perturbations from the planet. These arguments imply that the planet has a mass between that of Neptune and that of Saturn, a semi-major axis of approximately 119 AU and longitude of periastron and eccentricity, 0.1, the same as that of the ring edge.

Oral Session 11 Extrasolar Planets II

Wednesday, June 28, 2006, 10:20 am - 11:20 am

11.01 Dynamical Constraints on the Formation of Terrestrial Planets in Binary Star Systems

Elisa V. Quintana¹, F. C. Adams², J. J. Lissauer¹, J. E. Chambers³

¹*NASA Ames Research Center*, ²*University of Michigan, Ann Arbor*, ³*Carnegie Institution of Washington.*

The most common result from the star formation process is a binary star system. Disks have been observed in many young binary systems, and if planets form at the right places within such disks, they can remain dynamically stable for very long times. The mass and proximity of a stellar companion, however, can influence whether/where planetary accretion can occur around the primary star. We have performed a large number of simulations (~ 120) of the late stages of terrestrial planet formation around a solar type star, varying the stellar masses and the binary periastron, in order to make a brief survey of binary parameter space and to account for sensitive dependence on initial conditions in these dynamical systems. As expected, sufficiently wide binaries leave the planet formation process largely unaffected. As a rough approximation, binaries with periastron $q > 10$ AU, even for the extreme case of equal mass stars, have minimal effect on terrestrial planet formation within ~ 2 AU of the primary star. When the periastron value becomes as small as 5 AU, planets no longer form with $a = 1$ AU orbits and the mass distribution tilts toward $M < 1$ Earth-mass, i.e., the formation of Earth-like planets is compromised. Approximately 50% of the observed binaries have $q > 7$ AU, and given that the galaxy contains nearly 100 billion star systems, a large number of binaries are wide enough to allow both the formation and the long term stability of Earth-like planets.

11.02 Predictions For The Correlation Between Giant And Terrestrial Extrasolar Planets In Dynamically Evolved Systems

Dimitri Veras¹, P. J. Armitage¹

¹*Univ. of Colorado, Boulder.*

The large eccentricities of many giant extrasolar planets may represent the endpoint of gravitational scattering in initially more crowded systems. If so, the early evolution of the giant planets is likely to be more restrictive of terrestrial planet formation than would be inferred from the current, dynamically quiescent configurations. Here we study statistically the extent of the anti-correlation between giant planets and terrestrial planets expected in a scattering model. We use marginally stable systems of three giant planets, with a realistic range of planetary masses, as a

simple model for the initial conditions prior to scattering, and show that after scattering the surviving planets reproduce well the known extrasolar planet eccentricities beyond $a > 0.5$ AU. By tracking the minimum periastron values of all planets during the evolution, we derive the distribution of orbital radii across which strong perturbations (from crossing orbits) are likely to affect low mass planet formation. We find that scattering affects inner planet formation at orbital separations less than 50% of the final periastron distance of the innermost massive planet in approximately 30% of the realizations, and can occasionally influence planet formation at orbital separations less than 20% of the final periastron distance of the innermost massive planet. The domain of influence of the scattering massive planets increases as the mass differential between the massive planets decreases. Observational study of the correlation between massive and terrestrial extrasolar planets in the same system has the potential to constrain the origin of planetary eccentricity.

11.03 Stability Limits in Planetary Systems

Richard Greenberg¹, R. Barnes¹

¹Univ. of Arizona.

Stability of a planetary system can be defined in many ways. Two meaningful definitions, defined in the context of a system consisting of one star and two planets, are Lagrange stability and Hill stability. Lagrange stability requires that the planets remain bound to the star, conserves the ordering of the distance from the star, and limits the variations of orbital elements like semi-major axis and eccentricity. Hill stability is less stringent: It only requires that the ordering of the planets remain constant; the outer planet may escape to infinity. A region in orbital element space that is guaranteed to be Hill stable has been described analytically (Marchal and Bozis 1982, Gladman 1993), although Hill stable orbits may lie outside that region as well. No analytic criteria describe Lagrange stability, although it must be a subset of the Hill-stable space, by definition. We compare these analytical constraints with results of numerical integration of 1000 hypothetical planetary systems similar to the extra-solar systems 47 UMa and HD 12661 that had been performed by Barnes and Quinn (2004). All the results are consistent with the analytic constraint on Hill stability. Moreover, the numerically determined boundary for Lagrange stability lies close to the analytic boundary for Hill stability. This result is doubly interesting because the analytic limit was not developed for the Lagrange definition, and did not even define the boundary of Hill stability. Yet this agreement may have a practical application, if borne out by subsequent studies: It suggests an analytic formulation that may describe the criterion for Lagrange stability. This study also confirms that the planets in both the 47 UMa and the HD 12661 systems are about as closely packed as they can be, a result that, if generally true, may have important implications for planet formation.

Oral Session 12 Astrometry and Stellar Systems

Wednesday, June 28, 2006, 1:20 pm - 3:00 pm

12.01 Reconstructing Galaxy Orbits And Measuring Proper Motions From SIM.

Edward J. Shaya¹, A. Peel¹, P. J. Peebles², B. Tully³

¹Univ. of Maryland, ²Princeton U., ³Univ. of Hawaii.

There have been numerous improvements to the Numerical Action Method codes for reconstructing orbits with a standard cosmological context over the last 2-3 years. There have also been numerous (~200) high accuracy distance measurements of nearby galaxies, mostly from application of the TRGB method to HST observations. We will present recent findings on the state of the Local Group and nearby groups, the masses of nearby galaxies and the Virgo Cluster, and limits on hot and warm dark matter.

We will also discuss the potential for using SIM to measure proper motions of nearby galaxies to add 2 more phase-space constraints per galaxy and how this aids in improving solutions and solving for individual masses of galaxies.

12.02

Status Of Ucac And Urat Projects

Norbert Zacharias¹

¹U.S. Naval Observatory.

All-sky observing of the USNO CCD Astrograph Catalog (UCAC) program was completed in 2004. Reductions are in progress for the final release (UCAC3) which is expected to be distributed in early 2007. It will contain positions and proper motions of about 60 million stars for the 10 to 16 magnitude range with errors of 15 to 70 mas per coordinate (depending on magnitude) in positions and 1 to 6 mas/yr for proper motions. Reduction details including double star fits, catalog completeness and empirical PSFs will be discussed, as well as the type of products required by various users. Yet unpublished data of over 5000 astrograph plates which are being measured on StarScan will be incorporated into UCAC proper motions.

The USNO Robotic Astrometric Telescope will enter construction phase in 2006. This dedicated 0.85m aperture instrument will perform an all-sky survey to give 30 mas positions at 20th magnitude as well as positions, proper motions and parallaxes on the 5-10 mas level for stars in the 14 to 18 mag range. The world's largest monolithic detector, a 10.6k by 10.6 CCD is currently in production with Semiconductor Technology Associates (STA) and a complete prototype camera is expected by end of 2006.

12.03

Low-mass Binary Stars And The Mass-luminosity Relation: Past, Present, And Future

George F. Benedict¹, B. E. McArthur¹, T. J. Henry², O. G. Franz³, L. H. Wasserman³

¹Univ. of Texas, Austin, ²Georgia State University, ³Lowell Observatory.

The Mass-Luminosity Relation (MLR) is the second most important "map" of stellar astronomy, the H-R diagram being the first. The mass of a star is the key parameter that dictates its entire evolution. For single objects, the MLR allows astronomers to convert a relatively easily observed quantity, luminosity, to a more revealing characteristic, mass, yielding a better understanding of the object's nature. Additionally, determining precise masses for extrasolar planets requires knowing precise masses for their parent stars.

For the past ten years a group of us, led by Todd Henry, have carried out an investigation of the lower main-sequence MLR. Originally motivated by the immense scatter in that potentially very useful tool, we have obtained both fringe tracking and fringe-scanning observations of low-mass binary stars with the Hubble Space Telescope interferometric Fine Guidance Sensors. This project is one of, if not the longest ongoing General Observer project in the history of HST. In addition to FGS measures, we have carried out a radial velocity campaign on a number of these binary stars, using the Sandiford Echelle Spectrograph at the Struve 2.1m telescope at McDonald Observatory. The constraint that astrometry and radial velocities describe the same physical system improves the accuracy of our masses. This effort has resulted in a preliminary Mass-Luminosity relation made up of stars with mass errors typically 4%.

Ultimately we seek masses with 1% error. These will come from astrometry obtained with the Space Interferometry Mission (SIM). Such precision will improve comparisons with real stars, allowing choices to be made between various modeling approaches and the inclusion and modeling of stellar phenomena such as convection, mass loss, turbulent mixing, rotation, and magnetic activity. This work is supported by NASA grant STScI GO-10613 and SIM/JPL/GSU BLF57-02.

12.04 The Dynamical Challenges of the Polaris Multiple System

David G. Turner¹, I. A. Usenko², A. S. Miroschnichenko³, V. G. Klochkova⁴, V. E. Panchuk⁴, S. L. Yang⁵

¹Saint Mary's Univ., Canada, ²Odessa National University, Ukraine, ³University of North Carolina in Greensboro, ⁴Special Astrophysical Observatory, Russian Federation, ⁵University of Victoria, Canada.

The hierarchal triple system formed by the bright, nearby Cepheid Polaris, its visual companion (ADS 1477B), and recently resolved spectroscopic companion (ADS 1477Ab) at first sight seems well understood in terms of its astrometric properties: a parallax implying a distance of 132 ± 8 pc (Hipparcos), and residuals implying an orbital inclination of 50 degrees (Wielen et al. 2000). But the recent optical detection of ADS 1477Ab by Evans et al. (2005) with the Hubble Space Telescope can be used to place independent constraints on the orbital properties of the system, once it is combined with the parameters of the spectroscopic orbit. To that end, existing radial velocity data for Polaris over the past 120 years, including previously-unpublished and recent observations obtained over the past two decades, have been collected, reanalyzed, and examined in order to improve the orbital parameters for the spectroscopic binary. There are small discrepancies in the data that may be linked to different sets of spectral lines and wavelength coverage used to infer the photospheric motion of the Cepheid, or to the inevitable problems of establishing reliable systemic velocities for a pulsating star. But the primary discrepancies lie in the implied properties of the Polaris system from the orbital solution, which seem to confirm the parallax of Polaris but not the orbital inclination, which may be edge-on. The results also conflict directly with other features of Polaris that are inferred from its other Cepheid characteristics: decreasing light amplitude, rapid period increase, location near the center of the instability strip, and possible membership in the Pleiades moving group. Such discrepancies are numerous enough to raise suspicions that there may be a fourth star in the system, although its detection may defy observers.

12.05 On the Precision of Artificial Satellite Orbit Determination from Observations from an Orbiting Platform

Marc A. Murison¹

¹U.S. Naval Observatory.

This paper addresses the characterization of the precision of observationally determined orbit parameters when optical observations are taken of an artificial satellite (“target”) from another orbiting body (“platform”). Of interest are, among others, optimal platform orbits and optimal observing strategies for a given level of observational astrometric precision and for certain types of target orbits. Classical orbit determination methods are not particularly amenable for gaining analytical insight into the characterization of the determined orbital parameter errors. Here we make an attempt to bypass classical orbit determination and look for an approach that can instead make use of certain approximations to the relative distance and velocity vectors. Furthermore, given the modern possibility for spectroscopic optical instruments in space, we also investigate what may additionally be gained from radial velocity observations.

We start with the distance and velocity vectors of an orbiting target body with respect to an orbiting observation platform. We approximate the relative distance and velocity vectors, allowed by certain assumptions such as small eccentricities, relative inclination angle(s), and ratio of orbit radii. We then analytically propagate the observational errors through the equations and characterize what target orbit parameter errors we are able. It turns out this is more difficult than anticipated at first. We then perform numerical simulations to more completely characterize the behaviors of the determined orbit parameter errors.

Oral Session 13 Captures and Cataclysms
Wednesday, June 28, 2006, 3:20 pm - 5:00 pm

13.01 Did Lunar Trojans Cause the Lunar Cataclysm?

Matija Cuk¹, B. J. Gladman¹, J. Gallant¹

¹*Univ. of British Columbia, Canada.*

To study the fate of possibly-resonant debris in the early Earth-Moon system, we constructed a numerical integrator capable of simulating all aspects of the system's tidal evolution. We confirm (Canup et al. 1999) that bodies in exterior resonances are unstable, but find that tadpole orbits are generally long-lived, with eccentricities that decrease during outward evolution. Our integrations start with the Moon on a circular orbit at 5 Earth-radii with 11 degree inclination wrt Earth's equator. We also assume that the Lunar eccentricity tides dominated over dissipation in early Earth. When tides cause the Moon to spiral out to a distance of about 38-39 R_E, all the trojans escape due to an apparent resonance with the Sun. We identify this perturbation as the evection resonance (i.e. trojan orbital pericenters precessing once per year). Depending on the exact initial conditions the difference between the lifetimes of various trojans can be as large as 10% (with no significant asymmetry between L4 and L5) thus yielding two 'escape events' separated in time by up to hundred million years.

A Q value of 90 for early Earth would result in the trojan escape to be about 3.9 Byr ago, coincident with the epoch of the "Lunar Cataclysm" (Tera et al 1974). We thus propose that the cataclysm was caused by fragments of the two escaping Lunar trojans, which tidally disrupted and then collided with the Moon and Earth. The time spread of impacts from each of the two escape events would have been very brief (years for direct impacts, Myrs for impacts by bodies that escaped into heliocentric orbit). Uncertainties in the formation times of Lunar basins are sufficiently large that two distinct intense episodes may be consistent with the available cosmochemical chronology data.

13.02 The Fate of Debris Launched from the Galilean Satellites

Douglas P. Hamilton¹, D. B. Zeehandelaar¹

¹*Univ. of Maryland.*

A small fraction of interplanetary material moving at high speeds through the jovian system is intercepted by the Galilean satellites; the resulting energetic collisions chip bits of material off the moons and populate a diffuse torus of circumplanetary debris. We investigate the fate of this ejected material, focusing on both the transport probabilities between satellites and the steady-state spatial distribution of the material itself. Our goals are twofold. First we hope to quantify processes that deliver exotic compounds to satellite surfaces (e.g. sulfur from Io and possible organics from Europa). In addition, we seek an explanation for the 5-10 micron dust grains detected at high jovian latitudes by the two Pioneer spacecraft.

We find that large dust grains (> 20 microns) tend to keep either their pericenter or apocenter distances tied to the orbital radius of a Galilean satellite, while smaller micron-sized grains, dominated by strong non-gravitational forces including electromagnetism and radiation pressure, spread more evenly throughout the jovian system. Typical lifetimes for these grains are a few hundred years; large grains are typically lost to the satellites, while many small grains are also transferred to Jupiter. We find transitions to both interior and exterior satellites, although the former occur more readily. Our

integrations show that roughly 80%-90% of gravitationally-dominated ejecta returns to the source while the bulk of the remaining material is transferred to the nearest neighboring satellites. Particles of all sizes are scattered to high latitudes, and the 5-10 micron debris forms a distribution that readily accounts for the Pioneer detections.

13.03 **Satellite Capture via Binary-Planet Gravitational Encounters**

Craig Agnor¹, D. P. Hamilton²

¹University of California Santa Cruz, ²University of Maryland.

Given the observed prevalence (~1-10%) of gravitationally bound pairs in the asteroid and Kuiper belts and the variety of processes inherent to solar system evolution that create these pairs among the minor planets, three-body gravitational encounters between binaries and accumulating planets were a common occurrence in the early solar system. We have recently shown that Neptune's large satellite Triton may have been captured in just such an encounter (Agnor and Hamilton 2006). Here we will report on our efforts to extend this capture mechanism to other potentially captured planetary satellites. In particular we will discuss the binary characteristics and encounter dynamics needed for transfer between heliocentric and planetocentric orbits. We will also discuss this model of capture in context with planetary formation and satellite evolution.

13.04 **Three-Body Capture of Jovian Irregular Satellites**

Catherine McGleam¹, D. P. Hamilton¹, C. B. Agnor²

¹University of Maryland, ²University of California, Santa Cruz.

We numerically examine the capture of irregular satellites via three-body encounters between binary asteroids and Jupiter. To capture directly to an orbit similar to those of today's jovian irregulars requires a large primary, as suggested by H. Levison [1] and others. However, such objects were probably rare, even in the early Solar System. Here we consider an alternate path which eliminates the need for the massive primary. Our approach requires two sequential steps: 1) capture to a very distant orbit, and 2) weak orbital decay over a long timescale. The key is that capture is achieved almost immediately, while the orbital evolution can take place very slowly. This is unlike pull-down or gas drag capture, where the energy change is gradual and, if strong enough to capture a satellite, must cease soon afterwards to prevent collision with the planet. Because the orbital evolution is decoupled from the capture process, our mechanism does not require an especially large impulsive change to the speed during capture, and hence small binary components are viable.

Our four-body simulations include binaries of various characteristics, Jupiter, and the Sun. The binaries begin outside Jupiter's Hill sphere and approach on low-speed trajectories. We are currently investigating the prevalence of these low-approach-speed orbits from the nearby asteroid populations. Capture via this method is possible for all asteroid sizes, though smaller sizes require more specialized orbits. We find that Jupiter can acquire both prograde and retrograde satellites, and that capture is not strongly affected by the planet's orbital eccentricity. The Jacobi constant can be particularly valuable in proving that capture is permanent in cases where Jupiter follows a circular path.

We gratefully acknowledge support from the NASA Origins program.

[1] Levison, H., 2005. Private communication.

13.05 **Lifetimes of Small Bodies in Planetocentric (or Heliocentric) Orbits**

Anthony R. Dobrovolskis¹, J. L. Alvarellos², J. J. Lissauer³

¹UCO Lick Observatory / NASA Ames Research Center, ²Space Systems Loral, ³NASA Ames Research Center.

Small bodies left over from the formation of the planets and satellites litter the Solar System, along with the debris

from more recent collisions. These bodies are removed by expulsion from heliocentric or planetocentric orbit, as well as by collisions with planets, moons, and the Sun, with characteristic lifetimes depending on their orbits. However, the rate at which a given population of objects declines cannot be described by the simple exponential law used to describe radioactive decay. On the contrary, the removal of comets and remnant planetesimals has sometimes been described as “logarithmic decay”.

Our work on the fate of ejecta from Hyperion (Dobrovolskis and Lissauer 2004, Icarus 169, 462--473), as well as recent results from other satellites, suggests instead that ejecta removal is best described by a “stretched exponential” decay law, where the particle lifetimes increase as a fractional power of the elapsed time, suggestive of a diffusion process.

Statistical analysis supports this conclusion, and enables us to determine the decay parameters. The results should be valuable in several contexts, including the delivery of meteorites to Earth and the bombardment history of the planets and their moons.

Poster Session 14 Poster Session with refreshments

Wednesday, June 28, 2006, 5:10 pm - 6:40 pm

Posters will be displayed for the duration of the meeting.

14.01 Equilibria of Collisionless Systems

Eric Barnes¹, L. L. Williams¹, J. J. Dalcanton², A. Babul³

¹Univ. of Minnesota, ²Univ. of Washington, ³Univ. of Victoria, Canada.

We are investigating the nature of collisionless equilibria, particularly focusing on those structures that result from N-body simulations. There are several “universal” relations (density profile shape, density-velocity dispersion, density-anisotropy) that appear in such simulations and we are aiming to understand the relevant physical processes behind them. This work is supported through NSF AST-0307604.

14.02 Toward The Ultimate Accuracy Of The Global Astrometric Grid With The Space Interferometry Mission

Valeri V. Makarov¹, K. J. Johnston², N. Zacharias²

¹Caltech, ²USNO.

Global astrometric reference frames may be ultimately limited to ~ 1 micro-arcsecond accuracy by the effects of gravitational scintillation (stochastic microlensing), non-stationary gravitational bending of light in the Galactic potential, gravitational waves, acceleration of the Sun in the Galaxy, and acceleration of the Galaxy. The Space Interferometry Mission is expected to construct an optical reference frame to unprecedented accuracy based on a limited number of grid objects uniformly positioned across the sky. The global accuracy of this frame may be brought close to the ultimate threshold if the SIM grid is anchored to a number of extragalactic objects (mostly QSOs), whose positions can be considered fixed in the cosmological frame. These objects, observed by SIM alongside the regular grid stars, will help to constrain sky-correlated errors in parallaxes and, possibly, proper motions of science targets. They can be used to determine the residual position rotation of the SIM coordinate system and the residual spin of the proper motion system with respect to the quasi-inertial (non-rotating) extragalactic reference system. We estimate the gain in accuracy of the SIM astrometric grid and of the extragalactic tie, given realistic assumptions on the number and brightness of grid quasars, available mission time and observing schedule.

14.03

Bayesian Analysis of RR Lyrae Distances and Kinematics

W. H. Jefferys¹, T. R. Jefferys², T. G. Barnes³

¹*University of Vermont*, ²*Unaffiliated*, ³*University of Texas at Austin*.

We are using a hierarchical Bayes model to analyze the distances, luminosities, and kinematics of RR Lyrae stars. This model relates these characteristics to the raw data of proper motions, radial velocities, apparent luminosities and metallicities of each star. A combination of Gibbs and Metropolis-Hastings sampling, using latent variables for the actual velocity and luminosity of each star, is used to draw a sample from the full posterior distribution of these variables, and draw inferences on the quantities of interest in the usual way. We have applied our model to the much larger HIPPARCOS database, and we plan also to include metallicity in our model, which has not been done previously.

14.04

Anisotropic Turbulent Diffusion In Radiative Zones Of Stars

Nathalie Toque¹

¹*Saint Mary's University, Canada*.

Transport of chemical elements in radiative zone is always an open question in the theory of stellar evolution. Up to now, the standard model which takes into account the microscopic diffusion lacks to accurately predict the abundances anomalies at the top of the main sequence stars. Since more than ten years, other processes involving turbulence and waves are under investigation. But, the mechanism by which they increase or decrease the vertical diffusion of the chemical elements to the top of the star is not yet understood. At the beginning of the 90s, Chaboyer and Zahn (1992) proposed a model of turbulent diffusion coefficients assuming no overlap between the small and large turbulent scales. This last assumption was the main failure of the model and gave clues for the next studies. Vincent, Michaud et al (1996) made 2D simulations of anisotropic turbulence and showed that the vertical transport of a passive scalar is reduced when the vortices are more stretched in the horizontal direction than in the vertical one. Our work was to find again the results of Vincent et al by solving the Navier-Stokes equations under the Boussinesq approximation. We succeeded in. But, as it is usual in science, we faced new misunderstandings. For example, we found that the vertical transport of the tracer levels off in highly anisotropic turbulent flows. This stop was announced by previous studies and demonstrated with waves processes. But in our work, the Prandtl number is low enough to efficiently damp the gravity waves. The reduction of the vertical transport and the level off are only involved by sheared turbulence.

14.05

The Saturn Ring Spokes of September 2005

Colin J. Mitchell¹, C. C. Porco¹

¹*SSI/CICLOPS*.

The re-appearance of Saturn's ring spokes in September 2005 offers us a new opportunity to study the dynamics of the small dust grains believed to make up the spokes. These new spokes, which appeared in 3 Cassini ISS images taken of the dark side of the rings, have contrasts on the order of 20%, are approximately 6000 km in length and 1000 km wide, and appear nearly radial in the first image, indicating that they are likely quite young. Here we present our kinematic analysis of these new spokes as well as some preliminary results of our numerical simulations of the dynamics and electric charging of the dust grains comprising the spokes. We find that, due to the charge on these grains, their interactions with the planet's electric and magnetic fields cause their motions to deviate slightly from Keplerian.

14.06

Sampling Saturn's Rings with Weak Density Waves

Matthew S. Tiscareno¹, J. A. Burns¹, P. D. Nicholson¹, M. M. Hedman¹, C. C. Porco²

¹*Cornell Univ.*, ²*Space Science Institute.*

The unprecedented clarity of Cassini images of Saturn's rings allows the detection and analysis of a number of previously unobserved density waves, which are raised at inner Lindblad resonances (ILRs) with saturnian satellites. These waves, unlike the strong waves observed by Voyager, generally have strictly linear dispersion; that is, the induced density perturbations are much smaller than the background density. This enables the measurement not only of the rings' background surface density (which we quote at much higher precision than previous authors), but also the growth and damping of a wave's amplitude.

We employ a multi-step semi-automated process, based on the continuous wavelet transform, to model weak density waves observed in radial scans of Cassini images. Our results include the following:

- 1) In the mid-A Ring ($127,000 < r < 133,500$ km), the scatter in our background surface density measurements greatly exceeds our error bars, leading us to believe that it reflects real variations. This scatter, between 30 and 50 g/cm², is in fact somewhat smaller than that given by previous authors, but our error bars are considerably less.
- 2) In the inner A Ring ($r < 127,000$ km), by contrast, background surface density falls within a much narrower range, from 31 to 35 g/cm² for the 7 waves we analyzed.
- 3) Ring viscosity, which is derived from wave damping and which yields an upper limit on vertical thickness, consistently increases from the Cassini Division outward to the Encke Gap. Meaningful upper limits on the rings' vertical thickness can be quoted in the Cassini Division (3.0 m at $r \sim 118,800$ km, 4.5 m at $r \sim 120,700$ km) and the inner A Ring (10 to 15 m for $r < 127,000$ km).

14.07

The Secular Evolution of a Close Ring-Satellite System

Joseph M. Hahn¹

¹*Saint Mary's University, Canada.*

We use the rings model of Hahn (2003) to examine the secular evolution of a small satellite orbiting in a narrow gap in a dense planetary ring. The model shows that if the satellite has a small eccentricity, then its secular perturbations excites the eccentricities of the nearest ring particles orbiting at the gap edge. The ring's self-gravity then allows that disturbance to propagate outwards and across the ring in the form of a spiral density wave. Similarly, an inclined satellite also launches a spiral bending wave that propagates radially outwards from the gap's outer edge. When we use the rings model to consider Pan, which inhabits the Encke gap in Saturn's main A ring, we find that the satellite excites low amplitude spiral waves having very long wavelengths that are hundreds of km. Whether these low-amplitude waves might be observed by the Cassini spacecraft is also under investigation.

The excitation of these waves transmits angular momentum from the satellite to the ring, so this form of wave-action tends to damp the satellite's eccentricity and inclination. Note that the fates of a satellite's eccentricity and inclination are uncertain when it orbits in a gap. This is due to the competition between the satellite's many Lindblad resonances in the ring, which excites the satellite's eccentricity, and its corotation resonances, which might or might not damp its eccentricity (Goldreich and Tremaine 1980, Goldreich and Sari 2003). The satellite's inclination is also precarious, since its many vertical resonances in the ring tends to pump up the satellite's inclination (Borderies et al 1984). However, the rings model shows that the satellite's secular perturbation of the ring tends to damp its eccentricity and inclination at rates that dwarf the excitation mechanisms. The stability of the satellite's eccentricity and inclination thus seems assured.

14.08 Broken Time Symmetry In Dynamics Of Resonant Asteroids

Smilyana Dikova¹

¹Bulgarian Academy of Sciences, Bulgaria.

Among the most powerful statements in Science are those that mark absolute limits to the knowledge. In the present studies we study the ways in which the scientific paradigm of our days- Deterministic Chaos, shows the limit of our basic counting system and leads to a limited predictability of the long time dynamic evolution. We support a thesis according to which the breaking of the complete connection between cause and effect leads to a restricted utilization of the principle of causality. The broken Determinism supposes a new concept of time. We show how the elucidation of time paradox and resonance problem by the theory with broken time symmetry developed by the Ilya Prigogine Center for Nonlinear Phenomena and Statistical Physics permits us to define a principle of the so called “virtual causality”. We apply this principle to the modern challenge of Celestial Mechanics- the possibility for impacts between asteroids and the Earth. Our results show that chaotic behavior of the main belt resonance asteroids leads to a restricted prediction of their long term dynamic evolution. This means a principle uncertainty in impact predicting.

THURSDAY

Oral Session 15 Dynamical Modeling of Orbits

Thursday, June 29, 2006, 8:30 am - 10:20 am

15.011 The Quasi-Satellite Orbit: Theory and Examples

Paul Wiegert¹

¹*Univ. of Western Ontario, Canada.*

An asteroid moving around the Sun having the same mean motion and mean longitude as a planet, but a different eccentricity, remains near the planet much like a satellite even when the distance is large enough so that it is not a bound satellite in the strictest sense (eg. even when it is well outside the planet's Hill sphere). This motion, which we term "quasi-satellite" (QS) motion, is one class of possible behaviours of small bodies in 1:1 mean-motion resonance with a planet, of which Trojan or tadpole motion is perhaps the best known class. If the QS orbit is coplanar with the planet, then the motion is stable in the secular approximation. When the orbits are inclined enough, an asteroid can be trapped into such a quasi-satellite (QS) motion for a finite period of time. The conditions under which this can occur are discussed and examples of recently-discovered QS objects in our own Solar System are examined.

This work was supported in part by the Natural Sciences and Engineering Research Council of Canada.

15.02 An Advanced Manipulator For Poisson Series With Numerical Coefficients

Francesco Biscani¹, S. Casotto¹

¹*Universita' di Padova, Italy.*

The availability of an efficient and featureful manipulator for Poisson series with numerical coefficients is a standard need for celestial mechanics and has arisen during our work on the analytical development of the Tide-Generating-Potential (TGP). In the harmonic expansion of the TGP the Poisson series appearing in the theories of motion of the celestial bodies are subjected to a wide set of mathematical operations, ranging from simple additions and multiplications to more sophisticated operations on Legendre polynomials and spherical harmonics with Poisson series as arguments. To perform these operations we have developed an algebraic manipulator, called Piranha, structured as an object-oriented multi-platform C++ library. Piranha handles series with real and complex coefficients, and operates with an arbitrary degree of precision. It supports advanced features such as trigonometric operations and the generation of special functions from Poisson series. Piranha is provided with a proof-of-concept, multi-platform GUI, which serves as a testbed and benchmark for the library. We describe Piranha's architecture and characteristics, what it accomplishes currently and how it will be extended in the future (e.g., to handle series with symbolic coefficients in a consistent fashion with its current design).

15.03 A Scheme to Treat Properly Close Encounters in Perturbed Three-Dimensional Two-Body Problem using Levi-Civita Transformation in Osculating Orbital Plane

Toshio Fukushima¹

¹*Nat'l. Astron. Obs. of Japan, Japan.*

We present a scheme to treat properly close encounters in a three-dimensional two-body problem under perturbations. It is a combination of Sundman's time transformation and Levi-Civita's spatial coordinate transformation applied to the two-dimensional components of the position and velocity vectors in the osculating orbital plane. We

adopt a coordinate triad specifying the plane as a function of the orbital angular momentum vector only. Since the magnitude of the orbital angular momentum is explicitly computed from the in-the-plane components of the position and velocity vectors, only two components of the orbital angular momentum vector are to be determined. In addition to these, we select the total energy of the two-body system and the physical time as additional components of the new variables. The equations of motion of the new variables have no singularity even when the mutual distance is extremely small, and therefore, the new variables are suitable to deal with close encounters. As a result, the number of dependent variables in the new scheme becomes eight, which is significantly smaller than the existing schemes to avoid close encounters; by two than the Kustaanheimo-Stiefel and the Burdet-Ferrandiz regularizations, and by five than the Burdet-Heggie regularization.

15.04 Optimal Rendezvous Problem in a Central gravity Field with Drag.

Ashraf H. Owis¹

¹*Milano-Bicocca university, Italy.*

The work aims at solving the optimal feedback rendezvous problem for a spacecraft moving in a central field of gravity in addition experiencing air drag. We will use the generating function technique to solve the Hamilton-Jacobi-Bellman equation and compute the optimal control. We will discuss both the hard and soft boundary conditions.

Oral Session 16 Satellite Dynamics

Thursday, June 29, 2006, 10:40 am - 1:00 pm

16.01 On The Orbits And Masses Of The Satellites Of The Pluto-Charon System

Man Hoi Lee¹, S. J. Peale¹

¹*UC Santa Barbara.*

The orbits of the recently discovered satellites of Pluto, S/2005 P2 and S/2005 P1, are significantly non-Keplerian, even if P2 and P1 have negligible masses, because the mass ratio of Charon-Pluto is ~ 0.1 . We present an analytic theory with P2 and P1 treated as test particles. This analytic theory shows that the azimuthal periods of P2 and P1 are shorter than the Keplerian orbital periods and that the periaapse and ascending node of each of the satellites precess at nearly equal rates in opposite directions. The deviation from Kepler's third law is already detected in the unperturbed Keplerian fit of Buie and coworkers. We also present direct numerical orbit integrations with different assumed masses for P2 and P1 within the ranges allowed by the albedo uncertainties. If the albedos are as high as that of Charon, the masses of P2 and P1 are sufficiently low that their orbits are well described by the analytic theory. There is at present no evidence that P2 has any significant epicyclic eccentricity. However, the orbit of P1 has a significant epicyclic eccentricity, and its prograde periaapse precession with a period of 5300 days should be easily detectable. If the albedos are as low as that of comets, the large inferred masses induce significant variations in the epicyclic eccentricities and/or periaapse longitudes on the 400-500-day timescales, due to the proximity of P2 and P1 to the 3:2 mean-motion commensurability. In fact, for the maximum inferred masses, P2 and P1 may be in the 3:2 mean-motion resonance, with the resonance variable involving the periaapse longitude of P1 librating. Observations that sample the orbits of P2 and P1 well on the 400-500-day timescales should provide strong constraints on the masses of P2 and P1 in the near future.

16.02 **Excitation of Mercury's Free Libration in Longitude**

Stanton J. Peale¹

¹*UC, Santa Barbara.*

The variation in the Mercury's orbital elements from planetary perturbations excite a free libration in longitude (~ 10 year period) of the axis of minimum moment of inertia about the value (averaged over an orbit period) it would have had at any instant if the rotation rate were exactly uniform at 1.5 times the orbital mean motion. This excitation is due almost entirely to the small variations in the orbital semimajor axis. A free libration will persist in spite of damping by tidal and core-mantle dissipation, although the damping will ultimately limit the maximum amplitude. Because fluctuations in the amplitude on long time scales are large, the current amplitude of the free libration can only be used to place an upper bound on the magnitude of the dissipation. Forced librations (~ 60'' amplitude, 88 day period) are superposed on the free libration, and measurement of the latter for the determination of Mercury's core properties will not be compromised.

16.03 **Mimas And Enceladus Coorbitals: Where Are They?**

Apostolos Christou¹, M. H. Morais², F. Namouni³

¹*Armagh Obs., United Kingdom, ²GAUC-University of Coimbra, Portugal, ³CNRS-Observatoire de la Cote d'Azur, France.*

Trojan companions of planetary satellites are currently known to exist for the two saturnian moons Tethys and Dione but not for nearby Mimas and Enceladus.

To investigate the origin and causes of these observations, we have carried out long term numerical simulations of the saturnian satellites, both with and without tides, while we follow the evolution of an ensemble of test particles located in and around the satellites' coorbital regions. These simulations have provided vital clues on the mechanisms that help stabilise/destabilise coorbitals with the satellites Mimas, Enceladus, Tethys and Dione as well as the timescales over which these mechanisms operate. As a byproduct of this work, we have also measured the sensitivity of the Mimas-Tethys and Enceladus-Dione resonances to the integration parameters.

We will discuss these results and their implications for the existence and origin of trojan satellites in the saturnian system.

16.04 **The 2:1 Mean-motion Resonance between Proteus and Larissa**

Ke Zhang¹, D. P. Hamilton¹

¹*Univ. Of Maryland.*

Voyager 2 discovered six small satellites orbiting near Neptune; Proteus and Larissa, the two largest and outermost ones, display larger eccentricities than average, as well as non-zero inclinations. These satellites formed in a thin debris disk resulting from the catastrophic destruction of the original Neptunian satellites shortly after the capture of Triton. The slim debris disk suggests that moonlet orbits should not acquire significant tilts at formation, and any initial eccentricities should damp away rapidly due to tides. Hence, the non-zero eccentricities and inclinations of these two satellites require an explanation.

We investigate the possibility of mean-motion resonance passages as an excitation mechanism for the orbital eccentricities and inclinations of Proteus and Larissa. The most recent strong resonance between these two satellites, the 2:1, is located only ~600 km outside Larissa's orbit, or ~900 km inside Proteus'. This resonance probably occurred

only a few hundred million years ago. We find that not only is this resonance partially responsible for the current orbital shapes and orientations of the moons, but it also provides interesting constraints on their physical properties. Our study of this resonance limits the average density of the moons to $0.05 \text{ g/cc} < \rho < 1.5 \text{ g/cc}$, and puts a lower limit on their tidal quality factors, which parameterize energy loss due to tides: $Q > 10$.

Through numerical simulations, we identify a new type of three-body resonance between the small satellite pair and Triton. These resonances occur near the traditional 2:1 mean-motion resonances and, surprisingly, are much stronger than their two-body counterparts, presumably due to Triton's large mass and orbital inclination. We derive a mathematical framework to analyze resonances in this system, and discuss applications to extra-Solar planetary systems.

16.05 Dynamical Exploration of De Haerdtl Inequality between Ganymede and Callisto

Benoit Noyelles¹, A. Vienne¹

¹*IMCCE - Paris Observatory, France.*

We studied De Haerdtl great inequality 7:3 between the Galilean satellites Ganymede and Callisto and proved its high dynamical importance. We show that it induces chaos by Chirikov diffusion because of overlaps of several resonances. We identified these resonances thanks to a numerical frequency analysis.

This study is a first step to the elaboration of a scenario of dynamical evolution of the Galilean system, taking account of De Haerdtl inequality.

16.06 On the Theories of Bodily Tides. The Models and the Physics.

Michael Efroimsky¹, V. Lainey²

¹*U.S. Naval Observatory, ²l'Observatoire de Paris et l'Observatoire Royal de Belgique.*

The MacDonald-Kaula-Gerstenkorn theory of bodily tides assumes constancy of the geometric lag angle δ , while the Singer-Mignard theory asserts constancy of the time lag Δt . Each of these two models is tacitly based on a particular law of the geometric lag's dependence upon the main frequency χ of the tidal flexure. In the theory of Gerstenkorn (1955), MacDonald (1964), and Kaula (1964) $\delta \sim \chi^0$ while in the theory of Singer (1968) and Mignard (1979, 1980) $\delta \sim \chi^1$.

The actual dependence of the lag on the frequency is expected to be more complicated. Its functional form will be determined by the rheology of the planet. Each particular functional form of this dependence will unambiguously fix the form of the frequency dependence of the tidal quality factor, $Q(\chi)$. Since at present we know the shape of the function $Q(\chi)$, it enables us to reverse our line of reasoning and to single out the appropriate actual dependence $\delta(\chi)$. This dependence entails considerable alterations in the theory of tides.

16.07 Evidence for a Finite Obliquity of Europa From Cycloidal Cracks

Alyssa R. Sarid¹, T. A. Hurford², R. Greenberg³

¹*Dept. of Earth and Planetary Science, UC - Berkeley, ²NASA Goddard Space Flight Center, ³Lunar and Planetary Laboratory, Univ. of Arizona.*

Diurnally-varying tidal stress on Europa results in the formation of arcuate cracks called cycloids. Modeling of cycloids based on tidal stress has provided evidence for non-synchronous rotation of Europa and helped to constrain its rotation rate (Hoppa et al., *Science*, 285:1899-1902, 1999). While fits of cycloids have improved over time, some

observed features still cannot be fit using the diurnal stress model, even when stress accumulated during non-synchronous rotation is taken into account. In particular, observed cycloids that are near to or crossing the equator have not been modeled successfully in previous studies.

Recently it has been suggested that Europa has a non-zero obliquity of order 0.1° (Bills, Icarus, 175(1):233-247, 2005). Hurford et al. investigated the effects of obliquity on the stress field and generated global maps of hypothetical cycloids (LPSC abstract #13.03, 2006). They found that several of the observed attributes of the global cycloidal crack pattern, which were previously not reproducible, are natural results of stress from a small amount of obliquity ($\sim 0.1^\circ$). Here, we reexamine specific cycloids that lie near or across the equator. Previously we were unable to model these features, but inclusion of the stresses resulting from Europa's obliquity has allowed us to finally reproduce these cycloids. Our preliminary results indicate that no more than 0.5° of obliquity is required to fit these cycloids. Moreover, non-synchronous rotation is still required to explain how the cycloids have migrated from their formation longitudes to their current locations. Our results provide the first geologic evidence for a finite obliquity of Europa and confirm the likelihood of slow non-synchronous rotation. Including the effects of obliquity when modeling cycloids may lead to a more accurate determination of the non-synchronous rotation rate.

Author Index

- A'Hearn, M. F. **1.01I**
Adams, F. C. 11.01, **4.02**
Agnor, C. **13.03**
Agnor, C. B. 13.04
Alvarellos, J. L. 13.05
Armitage, P. J. 11.02
Babul, A. 14.01
Barnes, E. **14.01**
Barnes, R. 11.03, **3.03**
Barnes, T. G. 14.03
Bartlett, D. F. **4.04**
Benedict, G. F. **12.03**
Biscani, F. **15.02**
Bloch, A. M. 4.02
Bosh, A. 8.05
Burns, J. A. 14.06, 8.04, **8.05**
Cahill, M. **2.03**
Casotto, S. 15.02
Cassini-VIMS Team, 8.03
Catanzarite, J. **10.02**
Chakrabarty, D. **6.04**
Chambers, J. E. 11.01
Christou, A. **16.03**
Couchman, H. M. . P. **4.01I**
Cuk, M. **13.01**
Dalcanton, J. J. 14.01
de Pater, I. 7.01
Dikova, S. **14.08**
Dobrovolskis, A. R. **13.05**
Dones, L. 8.01
Efroimsky, M. **16.06**
Franz, O. G. 12.03
French, R. G. **8.01**
Fukushima, T. **15.03**
Gallant, J. 13.01
Gladman, B. J. 13.01
Greenberg, R. **11.03**, 16.07
Hahn, J. M. **14.07**
Hamilton, D. P. **13.02**, 13.03,
13.04, 16.04
Harris, A. W. **2.02**
Hayes, W. B. **3.01**
Hedman, M. 8.05
Hedman, M. M. 14.06, 8.03, 8.04
Henry, T. J. 12.03
Hurford, T. A. 16.07
Innanen, K. A. **6.02**
Jefferys, T. R. 14.03
Jefferys, W. H. **14.03**
Johansen, A. 3.04
Johnston, K. J. 14.02
Klochkova, V. G. 12.04
Lee, M. **16.01**
Lissauer, J. J. 11.01, 13.05
Lissauer, J. J. 3.03
Lissauer, J. J. 7.01
Majewski, S. R. **6.01I**
Makarov, V. V. **14.02**
Malhotra, R. **5.01I**
Marcy, G. W. **10.01I**
McArthur, B. E. 12.03
McGhee, C. 8.01
McGleam, C. **13.04**
Minchev, I. **6.03**
Miroshnichenko, A. S. 12.04
Mitchell, C. Jon. **14.05**
Morais, M. H. M. 16.03
Murison, M. A. **12.05**
Murray, N. 3.02
Namouni, F. 16.03
Nicholson, P. 8.05
Nicholson, P. D. 14.06, **8.03**, 8.04
Noyelles, B. **16.05**
Owis, A. H. **15.04**
Panchuk, V. E. 12.04
Peale, S. J. 16.01
Peale, S. J. **16.02**
Peebles, P. J. E. 12.01
Peel, A. 12.01
Porco, C. 8.05
Porco, C. C. 14.05
Porco, C. C. 14.06
Porco, C. C. 7.02
Porco, C. C. 8.04
Pravec, P. 2.02
Quillen, A. 6.03
Quillen, A. C. **10.03**
Quinn, T. R. 3.03
Quintana, E. V. **11.01**
Richardson, D. C. 2.01
Richardson, D. C. 3.03
Rudick, C. **4.03**
Salo, H. 8.01
Sarid, A. R. **16.07**
Scheeres, D. J. **1.03**
Shao, M. 10.02
Shaya, E. J. **12.01**
Showalter, M. 8.05
Showalter, M. R. **7.01**
Spitale, J. **7.02**
Statler, T. S. **1.02**
Stewart, G. R. **8.02**
Tanner, A. 10.02
Thommes, E. **3.02**
Tiscareno, M. 8.05
Tiscareno, M. S. **14.06**, **8.04**
Toque, N. **14.04**
Tully, B. 12.01
Turner, D. G. **12.04**
Unwin, S. 10.02
Usenko, I. A. 12.04
Veras, D. **11.02**
Vienne, A. 16.05
Walsh, K. J. **2.01**
Wasserman, L. H. 12.03
Watanabe, T. 1.02
Wiegert, P. **15.01I**
Williams, J. G. **9.01I**
Williams, L. L. R. 14.01
Yang, S. L. S. 12.04
Youdin, A. **3.04**
Yu, J. 10.02
Zacharias, N. **12.02**, 14.02
Zeehandelaar, D. B. 13.02
Zhang, K. **16.04**